Int J Clin Exp Med 2016;9(9):17377-17386
www.ijcem.com /ISSN:1940-5901/IJCEM0031241

Original Article

Therapy of C6 glioma with liposomal doxorubicin in rats: a MR diffusion-weighted imaging study

Chongyong Xu[1], Gui Zhang[2], Yaping Zhao[2], Yingzheng Zhao[3], Lijuan Chen[3], Aiqin Wu[2], Zhihan Yan[2], Guangbin Wang[1]

[1]Department of Radiology, Shandong Medical Imaging Research Institute Affiliated to Shandong University, Jinan, China; [2]Department of Radiology, Second Affiliated Hospital of Wenzhou Medical University, Wenzhou, China; [3]College of Pharmacy, Wenzhou Medical University, Whenzhou, China

Received April 26, 2016; Accepted July 30, 2016; Epub September 15, 2016; Published September 30, 2016

Abstract: Objective: This study aimed to evaluate the early efficacy of liposomal doxorubicin in the therapy of C6 glioma in rats by diffusion-weighted imaging. Methods: 24 male SD rats received implantation of C6 tumor cells. Tumor bearing rats were randomly assigned into therapy group and control group. Rats in therapy group received liposomal doxorubicin injection, while rats in control group received normal saline. Results: At 3 weeks, the tumor volume in control group and treatment group showed significant difference (P<0.01). At 2 weeks, the ADC at the tumor center was 0.74±0.08×10^{-3} and 1.08±0.07×10^{-3} mm^2/s in control group and treatment group, respectively, and the ADC at the tumor periphery was 0.60±0.05×10^{-3} and 0.83±0.07×10^{-3} mm^2/s, respectively, showing marked differences between groups (P<0.01). At 3 weeks, the ADC at the tumor center was 1.14±0.26×10^{-3} and 1.48±0.05×10^{-3} mm^2/s in control group and treatment group, respectively, and the ADC at the tumor periphery was 0.82±0.17×10^{-3} and 1.11±0.06×10^{-3} mm^2/s, respectively, showing significant differences between groups (P<0.01). In addition, the ADCs at tumor center and periphery at 2 and 3 weeks after cell implantation were significantly higher than those at 2 weeks in both groups (P<0.01). Conclusion: The ADC may reflect the microscopic change in glioma cell density and has a better efficiency in the prediction of therapeutic efficacy as compared to tumor volume. Liposomal doxorubicin is effective to treat rat C6 glioma. HE staining shows the tumor necrosis is more obvious and the viable cells reduce significant after treatment as compared to control group.

Keywords: Rats, glioma, diffusion magnetic resonance imaging

Introduction

Glioma is the most common primary tumor in the central nervous system and accounts for about 40% of primary intracranial tumor. Grade I glioma is benign, is often found in young people and has a low incidence. Grade II glioma is a common astrocytoma with diffuse invasion. Grade II glioma is an anaplastic astrocytoma. Grade IV glioma is glioblastoma and also known as malignant glioma which is highly malignant tumor in the brain with high invasiveness. Surgical resection of grade IV glioma is difficult and thus it has a high recurrence rate [1]. The prognosis of patients with grade IV glioma is very poor, even after chemotherapy and radiotherapy, the median survival time is only 10 months and the 2-year survival rate is lower than 10% [2, 3]. Currently, the efficacy of chemotherapy is poor for malignant glioma, and chemotherapy may also kill some normal cells, which significantly limit the effective therapy of tumors. Thus, to develop new strategies is crucial to increase the therapeutic efficacy and prolong the survival rate in glioma patients [4].

To understand the pathogenesis and development of glioma and to develop new and effective therapies for gliom, it is necessary to establish reliable animal model of glioma. Currently, 9L, F98, T9 and C6 cell lines are often used for the establishment of glioma animal model. Of these cell lines, C6 glioma animal model is convenient to be established, has a low cost and is easy to be popularized in experiments. Thus, it has been widely used in studies on glioma. C6 glioma cells with active cell proliferation were initially found in Wistar-Furth rats exposed to

N-nitroso-methylurea (MNU). To date, C6 cells have been successfully used to establish glioma animal model in Wistar rats, Sprague-Dawley rats and Long-Evans rats. In Wistar rats and Long-Evans rats, the glioma has clear borderline and complete capsule and is similar to brain metastatic tumor. However, in Wistar rats, glioma has some characteristics of malignant glioma, including nuclear pleomorphism, increased mitotic index, necrosis at tumor center, intra-tumor hemorrhage and invasion into brain parenchyma. On the basis of above finding, C6 glioma in Wistar rats is more similar to the natural malignant glioma [5].

Adriamycin is a broad spectrum antibiotic with anti-tumor activity and has been used in the treatment of some tumors. It has wide biochemical activities and potent cytotoxic activity. However, adriamycin has a lot of adverse effects such as cardiac toxicity, bone marrow suppression, gastrointestinal reaction and hair loss, which significantly limit its wide and long term use in clinical practice. In recent years, liposomes have been used as carriers of antitumor drugs, achieving favorable efficacy and currently, liposomal adriamycin is commercially available. Liposomes are bilayer vesicle structure composed of lipids such as phospholipids and cholesterol. They can bind to some receptors such as lipoproteins and glycoproteins. The preparation of liposomes is relatively easy and materials used in the preparation of liposomes have low toxicitiy and good biocompatibility. Liposome microbubbles refer to the microbubbles capsuled by monlayer phospholipids membrane and belong to lipid vesicles. They are not only used in the enhanced ultrasound, but may serve as targeted carriers of drugs. Capsulation of adriamycin with liposomes may increase its stability, delay its release, reduce its effective dose and free adriamycin concentration, increase the adriamycin concentration at the lesion site, decrease the accumulation of adriamycin at the sensitive site, increase the therapeutic efficacy and reduce its side effects. Thus, liposomal adriamycin has favorable in the therapy of glioma.

DQI is the unique non-invasive method used for the detection of water molecular movement in vivo. In clinical practice, DWI is widely used in the early diagnosis of brain infarction, especial for brain infarction in ultra early phase, which has been found to improve the prognosis of patients. DWI is also used in the differential diagnosis of diseases, staging of tumors [6], evaluation of therapeutic efficacy [7] and in animal studies [8]. In the present study, the technique developed by our group was used to prepare the liposomal adriamycin which was employed for the treatment of C6 glioma in rats and DWI was used to evaluate the therapeutic efficacy.

Materials and methods

Animals and grouping

24 male SD rats weighing 180-200 g were purchased from Experimental Animal Center of Wenzhou Medical University. Animals were housed for 1 week (body weight: 200-230 g) and the received intracranial implantation of C6 glioma. One week later, all the animals were confirmed to have tumor in the brain. Then, these rats were randomly assigned into therapy group (n=15) and control group (n=9). In brief, rats were intraperitoneally anethestized with 10% pentobarbital sodium at 0.5 ml/100 g. In therapy group, rats received injection of 10 μl/g liposomal adriamycin (prepared by the Prof Zhao in the College of Pharmacy of Wenzhou Medical College) via the tail vein once every other day. In control group, rats received injection of 10 μl/g normal saline once every other day. All the procedures were performed according to the Animal Care and Welfare Guideline.

MRI and related analysis

Routine and enhanced MRI: after intraperitoneal anesthesia with 10% pentobarbital sodium at 0.5 ml/100 g, rats were placed in a supine position. Signa 3.0T MR instrument (GE, USA) was used for MRI with a coil for rats (Shanghai Chenguang Company), and the tail was first imaged. Cross-sectional T1WI, coronal T1WI and enhanced T1WI were performed. The enhanced MRI was performed at 10 min after injection of 0.4 mmol/kg Gd-DTPA via the tail vein. Conditions for MRI: T1WI TR, 560 ms; TE, 27 ms, NEX, 2; matrix, 256×256; T2WI TR, 2300 ms; TE, 110 ms; NEX, 2; matrix, 256×256; slice thickness, 2.4 mm; slice interval, 2.9 mm, FOV, 56 mm×70 mm. MR DWI: DWI was done before enhanced MRI. Echo planar imaging (EPI) was employed with diffusion-sensitive factor (b) of 1000 s/mm^2, TR of 2300 ms and TE of

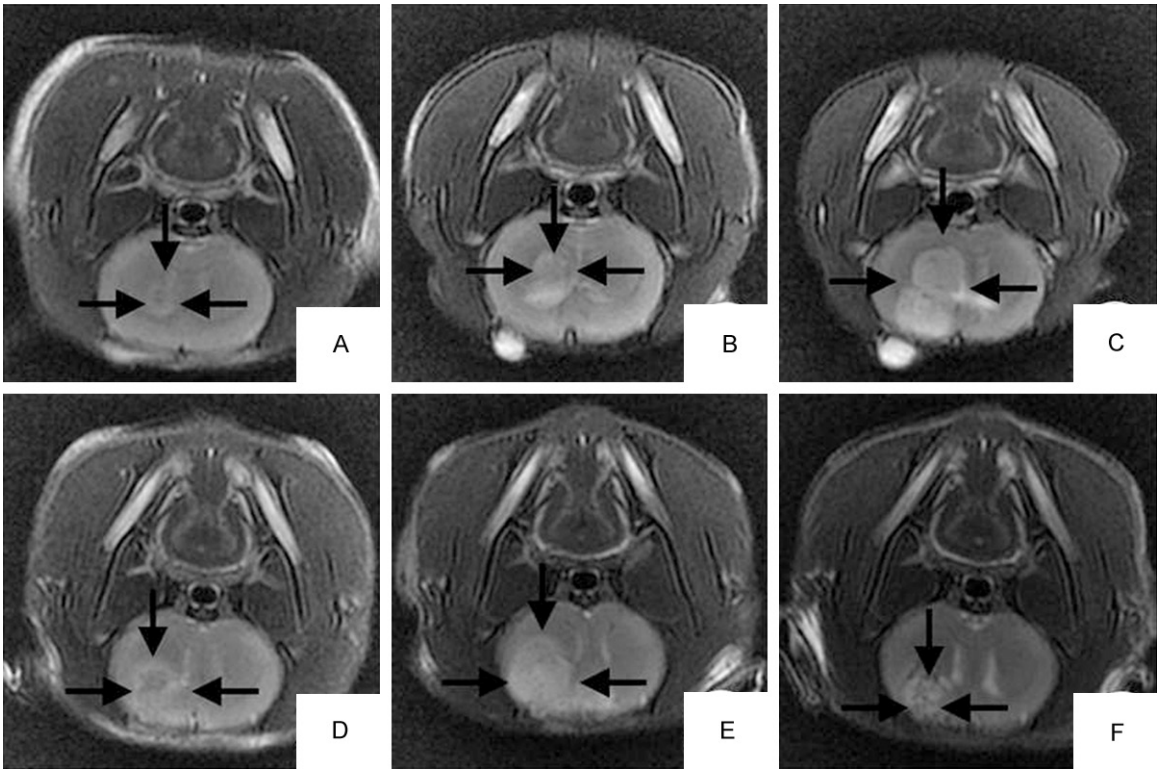

Figure 1. (A-C) T2WI cross section in control group at 1 (A), 2 (B) and 3 (C) weeks after implantation of C6 cells: oval hyperintense signals were observed at the right caudate nucleus and the tumor volume increased progressively. (D-F) T2WI cross section in therapy group at 1 (A), 2 (B) and 3 (C) weeks after implantation of C6 cells: oval hyperintense signals were observed at the right caudate nucleus and the tumor volume at 2 weeks (E) was larger than that at 1 week (D), but smaller than that at 3 weeks (F).

76 ms. The scanning site was determined according to the images of plan scanning. The slice thickness was 2.4 mm, slice interval was 2.9 mm, NEX was 2, matrix was 96×96 and FOV was 78 mm×130 mm. Parameters of MRI and analysis: (1) analysis of tumor volume (V) in enhanced MRI: The maximal length (L), width (W) and height (H) were measured at the maximum coronal and cross sections, and V was calculated as follow: $V = (4/3 \times \pi \times L \times W \times H) \times 1/8$ (unit: mm^3); (2) DWI analysis: the raw images were input into GE ADW4.3 station for analysis, recombination was done with b value, and color pseudo images of ADC were generated. At 2 and 3 weeks after implantation, 3 areas of interest (AOI) (2-3 mm^2) were independently selected at the center (the intersection between maximum length and its vertical line after enhanced scanning served as the inner borderline of AOI) and periphery (the periphery of enhanced tumor served as the outer borderline of AOI), and the average was obtained for the calculation of ADC.

Statistical analysis

IBM statistical product and service solutions (SPSS) 19.0 was employed for statistical analysis. Quantitative data with normal distribution are expressed as means ± standard deviation ($\bar{x} \pm s$) and those with abnormal distribution as medians. Normal distribution was tested with *Kolmogorov-Smirnov* test. The ADC before and after therapy and that between two sites in a specific group were compared with independent sample t test. The homogeneity of variance was tested with *Levene* test. Data with homogeneity of variance were compared with two sample t test; data with heterogeneity were compared with approximate t test. V before and after therapy were compared with independent sample rank sum test between two groups, and V before and after therapy in a specific group was compared with paired rank sum test. A value of $P<0.05$ was considered statistically significant.

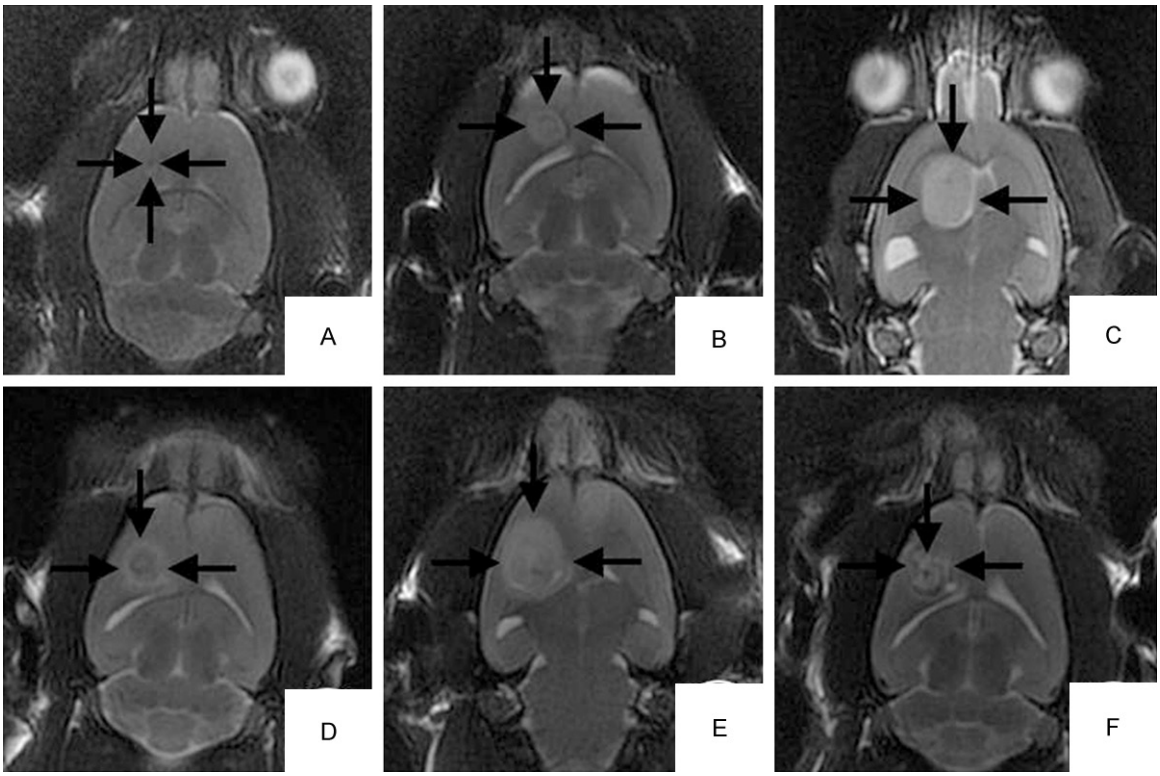

Figure 2. (A-C) T2WI coronal section in control group at 1 (A), 2 (B) and 3 (C) weeks after implantation of C6 cells: oval hyperintense signals were observed at the right caudate nucleus and the tumor volume increased progressively. (D-F) T2WI coronal section in therapy group at 1 (A), 2 (B) and 3 (C) weeks after implantation of C6 cells: oval hyperintense signals were observed at the right caudate nucleus and the tumor volume at 2 weeks (E) was larger than that at 1 week (D), but smaller than that at 3 weeks (F).

Results

MR findings

At 1 week after implantation, tumor was obtained in the brain of all 24 rats. Cord-like tumor was observed in the right caudate nucleus, and showed hypointese or equal intense signals in T_1WI and hyperintese signals in T_2WI. The tumor had a clear borderline with surrounding tissues, and the edema of surround tissues was not obvious (**Figures 1A** and **2A**). Even enhancement was observed in enhanced scanning, and liquefactive necrosis was not found (**Figure 3A**). In control group, the tumor volume increased progressive within 3 weeks after implantation, the ipsilateral ventricle was oppressed, the midline was pushed to right, mild liquefactive necrosis was found at 2 weeks (**Figure 3B**), the tumor had clear borderline with surrounding tissues and the edema of surrounding tissues was not obvious (**Figures 1B** and **2B**). At 3 weeks, mild liquefactive necrosis was noted in the tumor, mild edema of surrounding tissues was found, and the borderline between tumor and surrounding tissues was unclear (**Figure 1C**). In therapy group, the tumor volume at 2 weeks was larger than that at 1 week, mild edema of surrounding tissues was observed, and the borderline between tumor and surround tissues was unclear (**Figures 1E** and **2E**), significant enhancement was observed after enhanced scanning, and liquefactive necrosis was found in the tumor (**Figure 3E**). At 3 weeks, the tumor volume was significantly reduced as compared to that at 2 weeks, mild edema was also observed in the surrounding tissues, there was unclear borderline between tumor and surrounding tissues (**Figures 1F** and **2F**), and partial liquefactive necrosis was observed at the center of the tumor (**Figure 3F**). The tumor volume at different time points in both groups is shown **Table 1.** In therapy group, reduction in tumor volume was found in 14 rats and unchanged tumor volume was noted in 1 rat at 3 weeks as compared to the tumor volume at 2 weeks.

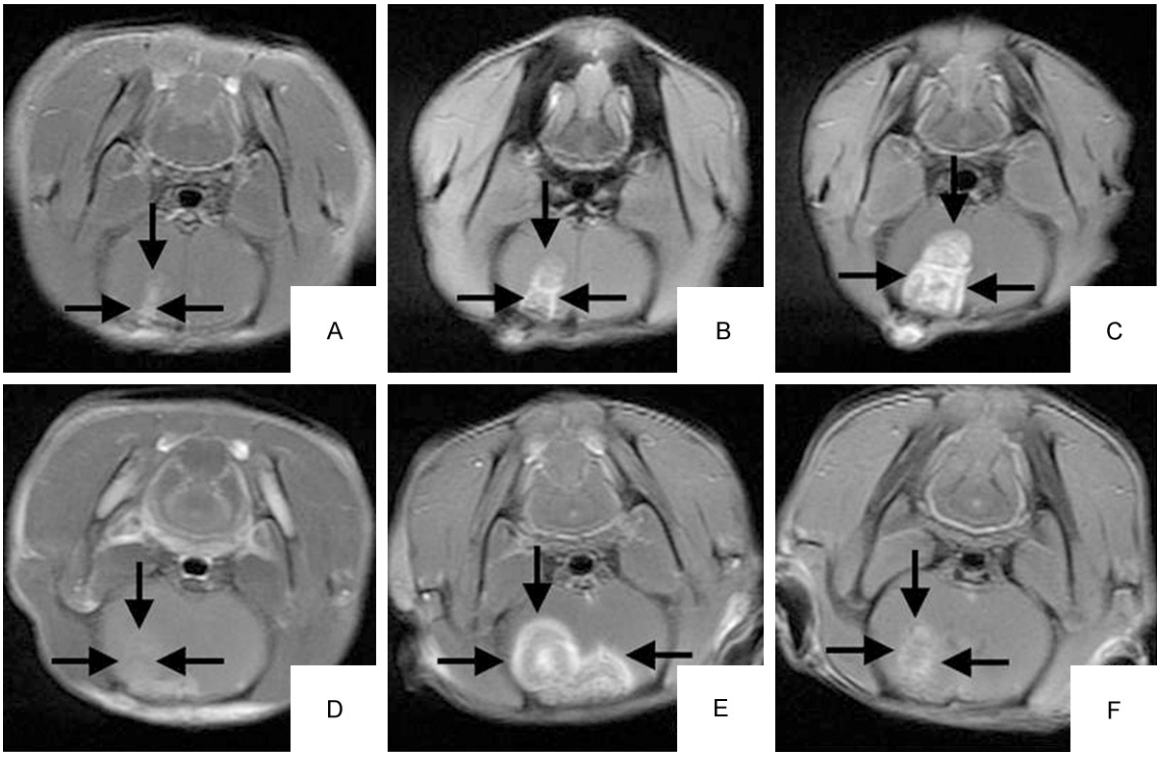

Figure 3. (A-C) T1WI cross section in control group at 1 (A), 2 (B) and 3 (C) weeks after implantation of C6 cells: cord like lesions with obvious enhancement were observed at the right caudate nucleus, evident liquefactive necrosis was not observed and the tumor volume increased progressively. (D-F) T1WI coronal section in therapy group at 1 (A), 2 (B) and 3 (C) weeks after implantation of C6 cells: oval hyperintense signals were observed at the right caudate nucleus and the tumor volume at 2 weeks (E) was larger than that at 1 week (D), but smaller than that at 3 weeks (F).

Table 1. Tumor volume in therapy group and control group at different time points (mm^3)

Group	2 weeks	3 weeks	*Z*	*P*
Control (n=9)	87.92	164.85	-2.67	<0.01
Therapy (n=15)	109.90	33.49	-3.41	<0.01
Z	-0.51	-3.46		
P	>0.05	<0.01		

Findings in DWI

In control group, after implantation, the tumor was unclear in DWI at 1 week, but showed even hyperintese signals higher (mainly blue in ADC image) than those in normal white matter in DWI at 2 weeks (**Figure 4A**). At 3 week, the tumor showed uneven hyperintese signals, patchy hypointense signals were observed at the tumor center (mainly green in ADC images) (**Figure 4B**). In therapy group, the tumor was unclear in DWI at 1 week, but showed hyperintese signals at the periphery and hypointese signals at the center (mainly blue-green in ADC images) (**Figure 4C**). At 3 weeks, patchy hypointense signals were observed in DWI, and tumor periphery showed circular hyperintese signals (mainly green-yellow in ADC images) (**Figure 4D**), but the tumor area reduced as compared to that at 2 weeks. The ADC at different areas and at different time points is shown in **Tables 2-5**.

Histological examination

HE staining was performed for histological examination. In control group, the tumor cells was dense and showed atypia, cell arrangement was disordered, small vessels were dilated in the surrounding tissues, tumor cells displayed invasive growth along the small vessels, tumor nest was also occasionally observed, cell nuclei were dark-stained, and patchy hemorrhage and necrosis were also occasionally observed between tumor cells (**Figure 5A**, **5B**). In therapy group, the tumor volume reduced, a large amount of patchy necrosis was observed

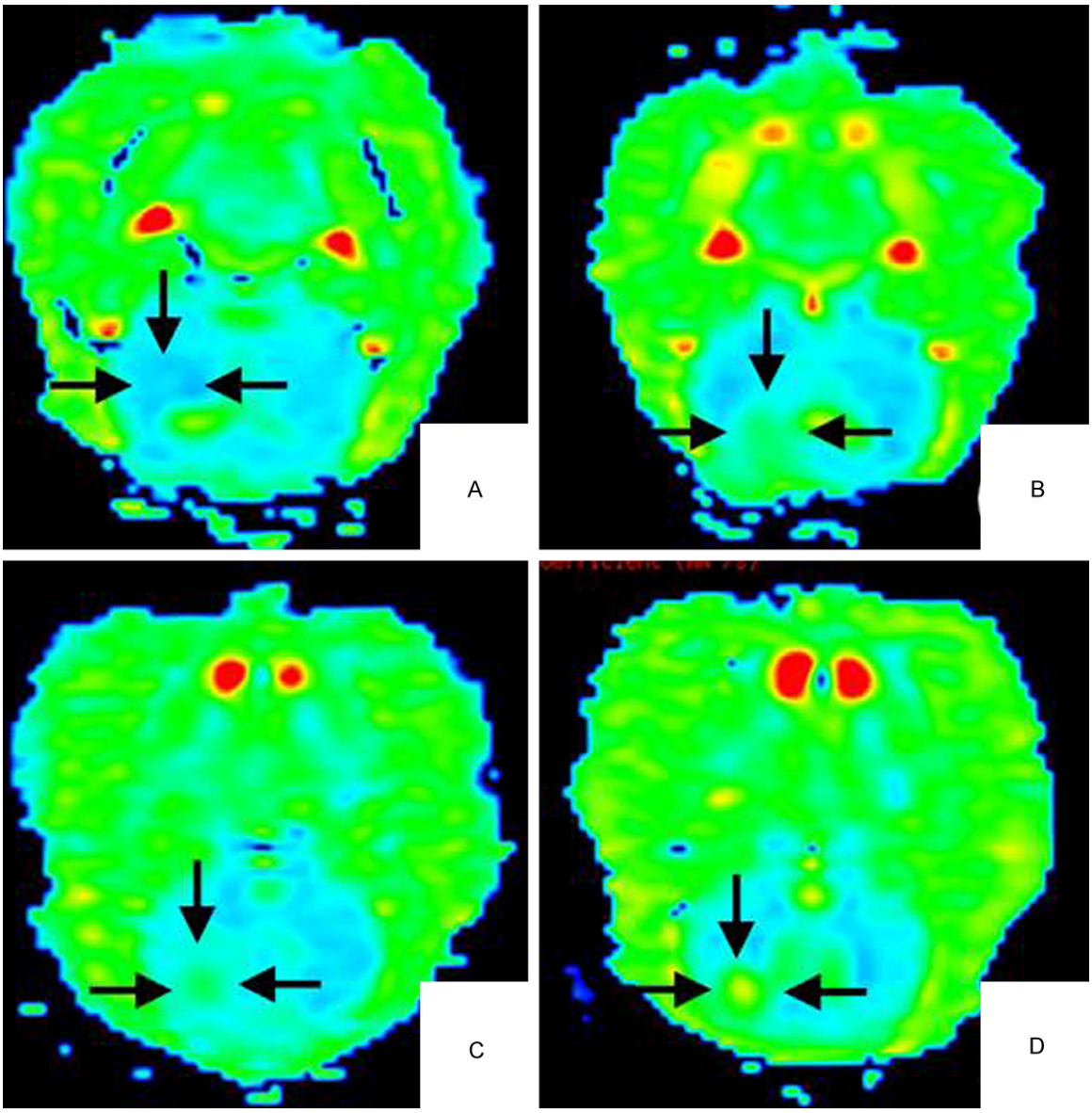

Figure 4. (A, B) ADC images at 2 and 3 weeks after implantation of C6 cells in control group. The lesions at the right caudate nucleus were mainly blue (A) at 2 weeks and mainly green (B) at 3 weeks. (C, D) ADC images at 2 and 3 weeks after implantation of C6 cells in therapy group. The lesions at the right caudate nucleus were mainly blue-green (C) at 2 weeks and mainly green-yellow (D) at 3 weeks.

at the tumor center, tumor cells became disrupted, and cell count reduced as compared to control group (**Figure 6A**, **6B**).

Discussion

Therapy of glioma with liposomal adriamycin

Adriamycin is a broad spectrum antibiotic with anti-tumor activity and has been used in the treatment of some tumors. It has wide biochemical activities and potent cytotoxic activity. However, adriamycin has cardiac toxicity and may cause progressive heart failure, or even death, which is often found in 2% of patients when the dose of adriamycin is as high as 450~500 mg/m^2. This significantly limits its wide application in clinical practice. The drug carrier may change the distribution of a specific drug and reduces its concentration in the heart, which also reduces its cardiac toxicity. In addition, adriamycin has other adverse effects such as bone marrow suppression, gastrointestinal

Table 2. ADC at different sites in both groups at 2 weeks after implantation ($\times 10^{-3}$ mm^2/s, $\bar{x} \pm s$)

Group	2 weeks			
	Center	Periphery	*t*	*P*
Control (n=9)	0.74±0.08	0.60±0.05	4.05	<0.01
Therapy (n=15)	1.08±0.07	0.83±0.07	9.82	<0.01
t	10.42	8.61		
P	<0.01	<0.01		

Table 3. ADC at different sites in both groups at 3 weeks after implantation ($\times 10^{-3}$ mm^2/s, $\bar{x} \pm s$)

Group	3 weeks			
	Center	Periphery	*t*	*P*
Control (n=9)	1.14±0.26	0.82±0.17	3.06	<0.01
Therapy (n=15)	1.48±0.05	1.11±0.06	17.94	<0.01
t	3.86	4.89		
P	<0.01*	<0.01*		

Note: *approximate *t* test.

Table 4. ADC at different sites and at different time points in control group ($\times 10^{-3}$ mm^2/s, $\bar{x} \pm s$)

Group	Control group			
	Center	Periphery	*t*	*P*
2 weeks	0.74±0.08	0.60±0.05	4.05	<0.01
3 weeks	1.14±0.26	0.82±0.17	3.06	<0.01
t	-6.26	-5.17		
P	<0.01	<0.01		

Table 5. ADC at different sites and at different time points in therapy group ($\times 10^{-3}$ mm^2/s, $\bar{x} \pm s$)

Group	Therapy group			
	Center	Periphery	*t*	*P*
2 weeks	1.08±0.07	0.83±0.07	9.82	<0.01
3 weeks	1.48±0.05	1.11±0.06	17.94	<0.01
t	-15.93	-18.85		
P	<0.01	<0.01		

reactions and hair loss, which significantly limit its wide and long term use in clinical practice. Liposomes are bilayer vesicle structure composed of lipids such as phospholipids and cholesterol. They can bind to some receptors such as lipoproteins and glycoproteins. Liposomes are good carriers of drugs and may change the biological distribution of adriamycin in vivo. Preclinical experiments and clinical trials have shown that liposomes may accumulate in tumors. The normal capillaries have complete vessel wall, and thus are impermeable to most liposomes. However, the capillaries in tumors usually show elevated permeability and are discontinuous with the intercellular space of about 100-780 nm. Thus, liposomes in the blood may enter the tumor via these spaces, which increases the adriamycin concentration in the tumor and leads to a slow release of adriamycin, leading to the elevated therapeutic efficacy [9]. Liposomal adriamycin prepared with different carriers not only reduces the cardiac toxicity of adriamycin, but increases the transportation of adriamycin in cells, which elevates the dose of adriamycin entering the intracranial tumor via the blood brain barrier. In addition, this also reduces the accumulation of liposomal adriamycin in the sensitive organs. These indicate that liposomal adriamycin has the potential in the therapy of glioma [10-12]. To date, liposomal adriamycin has been widely used in the combined therapy of tumors achieving favorable efficacy [13, 14].

MRI findings and pathological manifestations

In therapy group, rats received liposomal adriamycin treatment at 2 weeks after implantation of C6 glioma cells. In control group and therapy group, the tumor volume was 87.92 mm^3 and 109.90 mm^3 at 2 weeks and no significant difference was observed although the tumor volume in therapy group was larger than in control group. This may be explained as that the tumor volume in therapy group is larger than in control group at week 1, the effectiveness of liposomal adriamycin is not obvious within 1 week after therapy and thus it continues to grow within 1 week after therapy. When the anti-tumor effect was present, tumor cells became swelling, which may not immediately cause reduction in tumor volume. Different from tumor volume, the ADC was significantly different between two groups at 2 weeks. The ADC at different areas in therapy group was significantly higher than in control group. This may be explained as that liposomal adriamycin has cytotoxicity to tumor cells and thus cause cell apoptosis and necrosis, which reduce cell density, increase intercellular space and lead to the increase diffuse of water molecules, resulting in elevation of ADC. At 3 weeks, the tumor volume reduced as compared to that at 2 weeks in therapy group, but

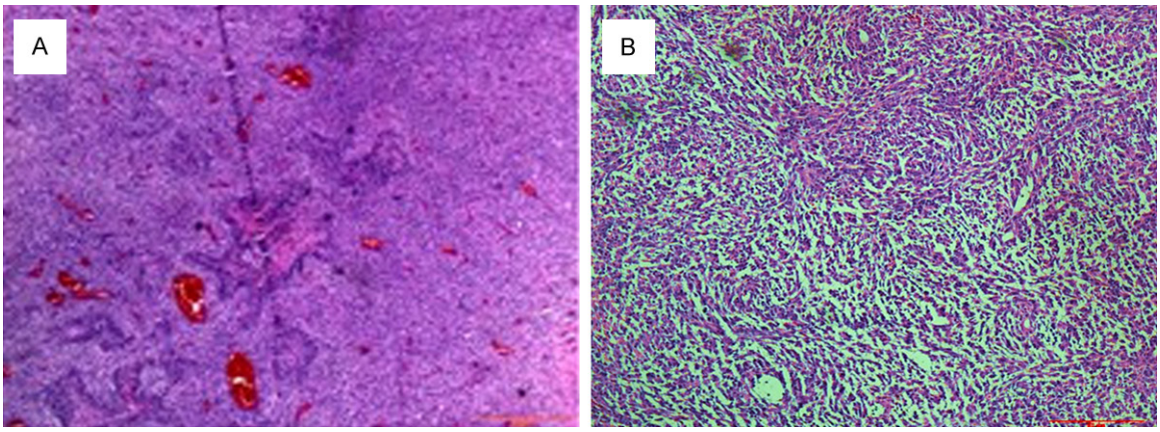

Figure 5. A, B: At 3 weeks, cell density in the tumor was high, cells showed atypia, cell arrangement was disordered, small vessels in surrounding tissues were dilated, tumor cells displaced invasive growth along the vessels, tumor nest was occasionally observed, cell nucleus was dark-stained, and hemorrhagic necrosis was also occasionally observed in the tumor.

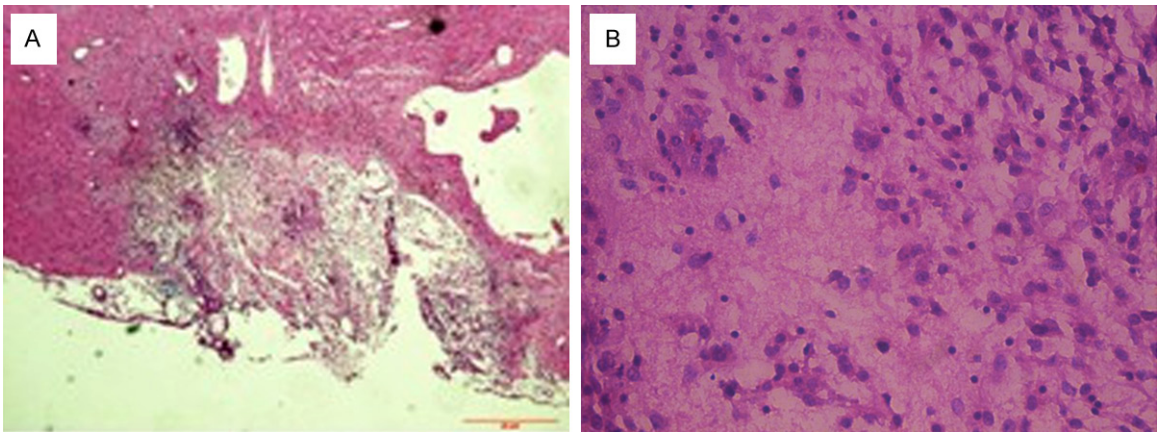

Figure 6. A, B: At 3 weeks, tumor volume reduced, massive patchy necrosis was observed at the tumor center, tumor cells became disrupted, and cell count reduced significantly in therapy group as compared to control group.

the tumor volume in control group increased at 3 weeks as compared to that at 2 weeks. In addition, ADC at different areas in therapy group was significantly higher than in control group. This may be explained as that a large amount of tumor cells become disrupted, cell count reduces and the intercellular space increases, leading to the elevation of water molecule diffusion and the increase in ADC. These were confirmed in pathological examination. Thus, we speculate that the change in ADC occurs earlier than the tumor volume dose and thus ADC is better to predict the therapeutic efficacy, which is consistent with previously reported in animal studies [15, 16]. In both groups, the ADC increased at 3 weeks as compared to that at 2 weeks. Generally, the tumor growth becomes more active over time, the tumor cell density also increases, and ADC at different areas reduces over time, which are inconsistent with our findings. In previous studies, Wistar rats were used, but SD rats were employed in the present study. C6 glioma cells were initially identified and separated from Wistar rats exposed to MNU. Thus, we speculate that SD rats initiate immunological rejection to C6 glioma cells. With the tumor growth, the tumor cells become apoptotic and necrotic, cell count reduces, intercellular space increases, water molecule diffusion increases, and thus ADC increases. In therapy group, the ADC at 3 weeks increased as compared to that at 2 weeks. This may be explained as that liposomal adriamycin has potent cytotoxicity to tumor

cells, which may cause cell apoptosis and necrosis at 3 weeks as compared to those at 2 weeks. Thus, cell density reduces, intercellular space increases, water molecule diffusion elevates and the tumor volume at 3 weeks reduces as compared to that at 2 weeks, suggesting the therapeutic effectiveness.

Glioma is the most common primary tumor of the central nervous system and has the characteristic of active growth at periphery. Thus, in this study, ADC was measured at the center and periphery of the tumor. Results showed the ADC at the center was significantly higher than that at the periphery in both group. As shown in histological examination, the cell density at the tumor periphery was higher than that at the center. Thus, the signal difference in ADC images may indirectly reflect the microscopic cell density of glioma.

Conclusion

The signal difference in ADC images may indirectly reflect the microscopic cell density of glioma. The change in ADC of glioma after therapy occurs earlier as compared to tumor volume. Liposomal adriamycin is effective for the therapy of C6 glioma in rats, and it may cause more obvious necrosis and reduce cell count at the tumor center as compared to control group.

Disclosure of conflict of interest

None.

Address correspondence to: Guangbin Wang, Department of Radiology, Shandong Medical Imaging Research Institute Affiliated to Shandong University, Jinan, China. E-mail: wgb7932596@hotmail.com; Yaping Zhao, Department of Radiology, Second Affiliated Hospital of Wenzhou Medical University, Wenzhou, China. E-mail: 939655548@qq.com

References

[1] Li K, Han H, Zhu K, Lee K, Liu B, Zhou F, Fu Y and He Q. Real-time magnetic resonance imaging visualization and quantitative assessment of diffusion in the cerebral extracellular space of C6 glioma-bearing rats. Neurosci Lett 2013; 543: 84-89.

[2] Lu C and Shervington A. Chemoresistance in gliomas. Mol Cell Biochem 2008; 312: 71-80.

[3] Verreault M, Strutt D, Masin D, Anantha M, Yung A, Kozlowski P, Waterhouse D, Bally MB and Yapp DT. Vascular normalization in orthotopic glioblastoma following intravenous treatment with lipid-based nanoparticulate formulations of irinotecan (Irinophore C), doxorubicin (Caelyx(R)) or vincristine. BMC Cancer 2011; 11: 124.

[4] Yang FY, Wong TT, Teng MC, Liu RS, Lu M, Liang HF and Wei MC. Focused ultrasound and interleukin-4 receptor-targeted liposomal doxorubicin for enhanced targeted drug delivery and antitumor effect in glioblastoma multiforme. J Control Release 2012; 160: 652-658.

[5] Stan AC, Casares S, Radu D, Walter GF and Brumeanu TD. Doxorubicin-induced cell death in highly invasive human gliomas. Anticancer Res 1999; 19: 941-950.

[6] Choi HS, Kim AH, Ahn SS, Shin NY, Kim J and Lee SK. Glioma grading capability: comparisons among parameters from dynamic contrast-enhanced MRI and ADC value on DWI. Korean J Radiol 2013; 14: 487-492.

[7] Pieper CC, Sprinkart AM, Meyer C, Konig R, Schild HH, Kukuk GM and Murtz P. Evaluation of a Simplified Intravoxel Incoherent Motion (IVIM) Analysis of Diffusion-Weighted Imaging for Prediction of Tumor Size Changes and Imaging Response in Breast Cancer Liver Metastases Undergoing Radioembolization: A Retrospective Single Center Analysis. Medicine (Baltimore) 2016; 95: e3275.

[8] Zhang Z, Yuan Q, Zhou H, Zhao D, Li L, Gerberich JL and Mason RP. Assessment of tumor response to oxygen challenge using quantitative diffusion MRI in an animal model. J Magn Reson Imaging 2015; 42: 1450-1457.

[9] Abraham SA, Waterhouse DN, Mayer LD, Cullis PR, Madden TD and Bally MB. The liposomal formulation of doxorubicin. Methods Enzymol 2005; 391: 71-97.

[10] Wohlfart S, Khalansky AS, Gelperina S, Maksimenko O, Bernreuther C, Glatzel M and Kreuter J. Efficient chemotherapy of rat glioblastoma using doxorubicin-loaded PLGA nanoparticles with different stabilizers. PLoS One 2011; 6: e19121.

[11] Pang Z, Gao H, Yu Y, Guo L, Chen J, Pan S, Ren J, Wen Z and Jiang X. Enhanced intracellular delivery and chemotherapy for glioma rats by transferrin-conjugated biodegradable polymersomes loaded with doxorubicin. Bioconjug Chem 2011; 22: 1171-1180.

[12] Chen H, Qin Y, Zhang Q, Jiang W, Tang L, Liu J and He Q. Lactoferrin modified doxorubicin-loaded procationic liposomes for the treatment of gliomas. Eur J Pharm Sci 2011; 44: 164-173.

[13] Cheng D, Cao N, Chen J, Yu X and Shuai X. Multifunctional nanocarrier mediated co-delivery of doxorubicin and siRNA for synergistic en-

hancement of glioma apoptosis in rat. Biomaterials 2012; 33: 1170-1179.
[14] Fan Y, Du W, He B, Fu F, Yuan L, Wu H, Dai W, Zhang H, Wang X, Wang J, Zhang X and Zhang Q. The reduction of tumor interstitial fluid pressure by liposomal imatinib and its effect on combination therapy with liposomal doxorubicin. Biomaterials 2013; 34: 2277-2288.
[15] Chenevert TL, Stegman LD, Taylor JM, Robertson PL, Greenberg HS, Rehemtulla A and Ross BD. Diffusion magnetic resonance imaging: an early surrogate marker of therapeutic efficacy in brain tumors. J Natl Cancer Inst 2000; 92: 2029-2036.
[16] Roth Y, Tichler T, Kostenich G, Ruiz-Cabello J, Maier SE, Cohen JS, Orenstein A and Mardor Y. High-b-value diffusion-weighted MR imaging for pretreatment prediction and early monitoring of tumor response to therapy in mice. Radiology 2004; 232: 685-692.